Virology 484 (2015) 323–333

Contents lists available at ScienceDirect

Virology

journal homepage: www.elsevier.com/locate/yviro

Loss of marginal zone B-cells in $SHIV_{SF162P4}$ challenged rhesus macaques despite control of viremia to low or undetectable levels in chronic infection

Thorsten Demberg [a], Venkatramanan Mohanram [a], Thomas Musich [a], Egidio Brocca-Cofano [a,1], Katherine M. McKinnon [b], David Venzon [c], Marjorie Robert-Guroff [a,*]

[a] Section on Immune Biology of Retroviral Infection, Vaccine Branch, National Cancer Institute, Bethesda, MD 20892, United States
[b] FACS Core, Vaccine Branch, National Cancer Institute, Bethesda, MD 20892, United States
[c] Biostatistics and Data Management Section, National Cancer Institute, Bethesda, MD 20892, United States

ARTICLE INFO

Article history:
Received 17 April 2015
Returned to author for revisions
16 June 2015
Accepted 17 June 2015
Available online 4 July 2015

Keywords:
Rhesus macaque
Simian–human immunodeficiency virus infection
Marginal zone B cells
B cell dysregulation

ABSTRACT

Marginal zone (MZ) B cells generate T-independent antibody responses to pathogens before T-dependent antibodies arise in germinal centers. They have been identified in cynomolgus monkeys and monitored during acute SIV infection, yet have not been well-studied in rhesus macaques. Here we characterized rhesus macaque MZ B cells, present in secondary lymphoid tissue but not peripheral blood, as $CD19^+$, $CD20^+$, $CD21^{hi}$, IgM^+, $CD22^+$, $CD38^+$, $BTLA^+$, $CD40^+$, $CCR6^+$ and $BCL\text{-}2^+$. Compared to healthy macaques, $SHIV_{SF162P4}$-infected animals showed decreased total B cells and MZ B cells and increased MZ B cell Ki-67 expression early in chronic infection. These changes persisted in late chronic infection, despite viremia reductions to low or undetectable levels. Expression levels of additional phenotypic markers and RNA PCR array analyses were in concert with continued low-level activation and diminished function of MZ B cells. We conclude that MZ B-cell dysregulation and dysfunction associated with SIV/HIV infection are not readily reversible.

Published by Elsevier Inc.

Introduction

HIV infection profoundly affects B-cell functions leading to dysregulation. Compared to the partial reversal of $CD4^+$ T-cell loss in the periphery and gut mucosa by ART therapy, B-cell dysregulation is not fully reversed (D'Orsogna et al., 2007; Moir and Fauci, 2009; Regidor et al., 2011), although early ART may help prevent it (Moir et al., 2010). B-cell dysregulation occurs early after HIV and SIV infection, usually before $CD4^+$ T-cells decline, and strikingly manifests itself by skewing memory populations (Chagnon-Choquet et al., 2014; Kuhrt et al., 2010; Titanji et al., 2010, 2014). Additional broader effects of HIV infection on B-cells have been recently reviewed (Moir and Fauci, 2009).

Little is known about the effect of chronic HIV/SHIV infection on marginal zone (MZ) B-cells. MZ B-cells are a subset of B-cells found in secondary lymphoid organs that are responsible for an early antibody response to blood-borne pathogens (Lopes-Carvalho et al., 2005). Thus, they bridge innate and later occurring adaptive responses (Cerutti et al., 2013). MZ B cells may play important roles in HIV/SIV infection. They express high levels of complement receptor 2 (CR2/CD21) and thus can capture immune complexes efficiently. In addition the engagement of CD21 lowers the B-cell activation threshold (Carroll and Isenman, 2012). Cytokine and antibody production may also contribute to viremia control. In fact, maintenance of IL-10 and lymphotoxin-α levels in peripheral blood MZ-like B cells was associated with control of HIV-1 disease progression (Chagnon-Choquet et al., 2014). On the other hand, complement receptor 2 expression might contribute to establishment of an extracellular HIV reservoir in lymph nodes by capturing and maintaining HIV trapped in the form of immune complexes (Ho et al., 2007). HIV trapped on B-cells has been shown to remain infectious in an in-vitro infectivity assay (Moir et al., 2000). Therefore it is important to further elucidate the role and contributions of marginal zone B-cells in HIV/SHIV pathogenesis.

Here we have extensively phenotyped MZ B cells in rhesus macaques, and have examined this B cell subpopulation before and after infection with $SHIV_{SF162P4}$ in order to gain insight into its potential contribution to infection outcome. It has been reported that cynomolgus monkey MZ B cells are dysregulated and diminished in function

* Corresponding author at: NIH, NCI, Building 41, Room D804, Bethesda, MD 20892-5065, United States. Tel.: +1 301 496 2114; fax: +1 301 402 0055.
E-mail address: guroffm@mail.nih.gov (M. Robert-Guroff).
[1] Present address: University of Pittsburgh, Center for Vaccine Research, Pittsburgh, PA 15261, United States.

http://dx.doi.org/10.1016/j.virol.2015.06.022
0042-6822/Published by Elsevier Inc.

during early SIV infection (Peruchon et al., 2009). The SHIV-infected macaques exhibited control of viremia to low or undetectable levels over the course of disease progression, providing an opportunity to determine whether MZ B cell dysregulation is persistent or reversed with viremia control.

Results

Phenotype of rhesus macaque MZ B cells

MZ B cells of cynomolgus monkeys were previously reported to be CD21^{hi}, CD27$^{-/+}$ (Vugmeyster et al., 2004). We confirmed the presence of the CD21^{hi} phenotype in LN and spleen of rhesus macaques, but not in PBMC (Fig. 2). The average mean fluorescent intensity (MFI) for CD21 on naïve CD21^{+} splenic B-cells was 5785 whereas for MZ B-cells it was 39620 (6.8-fold higher). We confirmed low-level expression of CD27 on MZ B cells, but would classify them as CD27$^{-/dim}$ (Fig. 2A) based on a comparison of CD27 MFIs between MZ-B-cells (MFI of 410), resting (CD21^{+}CD27^{+}) B-cells (MFI of 1387) and naïve (CD21^{+}CD27^{-}) B-cells (MFI of 183).

We further phenotyped the cells and documented expression of additional B-cell markers (Table 2). The most highly and consistently expressed surface markers aside from CD19, CD20, and CD21, were IgM, CD22, BTLA, CD40, CD38, CCR6 and BCL-2. Over 90% of all CD21^{hi} B-cells were positive for these markers (Table 2). Over 80% of CD21^{hi} B-cells were also positive for IgD and HLA-DR (Table 2). Based on these data, we characterize rhesus macaque MZ B-cells as CD19^{+}, CD20^{+}, CD21^{hi}, IgM^{+}, CD22^{+}, CD38^{+}, BTLA^{+}, CD40^{+}, CCR6^{+} and BCL-2^{+} with some variation in expression of IgD and HLA-DR.

Influence of SHIV viremia on MZ B cells

Initially we examined MZ B cells in LNs of macaques early in chronic infection. The infected previously vaccinated and control animals showed no differences in viral loads (Fig. 1) and were therefore treated as a single group (see Materials and methods section). Comparing samples obtained prior to study initiation with those obtained 8 weeks post-infection we observed a decline in total B cells together with a significant drop in MZ B-cells ($p=0.023$ and 0.021, respectively; Fig. 3A and B). Correlation analysis indicated a weak trend in the decline in LN MZ B cells with plasma viral load ($r=0.43$; Fig. 3C). We also observed significantly increased expression of Ki-67 8 weeks post-infection compared to pre samples ($p<0.0001$; Fig. 3D), directly correlated with viremia ($r=0.66$; Fig. 3E). Surface expression of three additional markers was examined. LN MZ B-cells post-infection downregulated CD22 (Siglec-2) expression ($p<0.0001$, Fig. 3F), upregulated IgD ($p<0.0001$, Fig. 3G), and expressed high levels of CD38, a marker highly expressed on human plasma cells, although the proportion of positive cells was slightly downregulated post-infection ($p=0.028$, Fig. 3H). CD38 expression by MFI was significantly higher on MZ B-cells (CD21^{hi}) compared to naïve (CD21^{+}CD27^{-}) ($p<0.01$) or resting (CD21^{+}CD27^{+}) B-cells ($p<0.0001$) (mean MFI values of 5699, 5003, and 3088, respectively). However the MFI of CD38 pre and post-infection was unchanged (data not shown).

We next examined macaque B cells late in the chronic phase of SHIV$_{SF162P4}$ infection. The percentages of B-cells in circulation (PBMC) were not different between infected and uninfected macaques (Fig. 4A). However as reported for HIV infected humans (Chagnon-Choquet et al., 2014; Titanji et al., 2014) we saw significant skewing of memory B-cell subsets between healthy and chronically infected animals (Fig. 4B). In infected animals, naïve B cells were decreased and activated memory B cells increased compared to healthy animals ($p=0.0081$ for each). In contrast, a surprising decline in total splenic B cells in SHIV-infected animals was seen ($p=0.048$, Fig. 4C), in concert with the decline seen early in chronic phase in LN (Fig. 3A). Similarly, a drop in splenic MZ B cells was observed ($p=0.028$, Fig. 4D). We could not determine if as with the LN cells, this decline was correlated

Table 1
Antibody clones and colors used for flow cytometry.

Antigen	Color	Clone	Host species	Isotype	Supplier
CD2	Qdot605	S5.5	Mouse	IgG_2a	Invitrogen
CD3	BV605	SP34-2	Mouse	IgG_1,λ	BD Bioscience
CD14	Qdot605/Qdot800	Tu14	Mouse	IgG_2a	Invitrogen
CD19	PeCy5	J3-119	Mouse	IgG_1	Beckman Coulter
CD20	eF650NC	2H7	Mouse	IgG_2b,κ	eBioscience
CD21	PeCy7	B-ly4	Mouse	IgG_1,κ	BD Bioscience
CD22	Pe	RFB-4	Mouse	IgG_1	Invitrogen
CD23	APC	M-L233	Mouse	IgG_1,κ	BD Bioscience
CD27	PerCP-eF710	O323	Mouse	IgG_1,κ	eBioscience
CD38	FITC	AT-1	Mouse	IgG_1	Stem Cell Technologies
CD40	Ax700	5C3	Mouse	IgG_1,κ	BD Bioscience
CD69	APC-Cy7	FN50	Mouse	IgG_1,κ	Biolegend
CD86	APC	IT2.2	Mouse	IgG_2b,κ	Biolegend
CD95	FITC	DX2	Mouse	IgG_1,κ	BD Bioscience
CD184 (CXCR4)	BV421	12G5	Mouse	IgG_2a,κ	Biolegend
CD196 (CCR6)	Pe	11A9	Mouse	IgG_1,κ	BD Bioscience
CDw199 (CCR9)	FITC	112509	Mouse	IgG_2a	R&D Systems
CD257 (BAFF/BlyS)	Pe	T7-241	Mouse	IgG_1,κ	Biolegend
CD272 (BTLA)	Pe	J168-540	Mouse	IgG_1,κ	BD Bioscience
α4β7	APC	A4B7	Rhesus recombinant	IgG_1	NHP Reagent Resource
IgD	Texas Red[a]	Polyclonal	Goat	NA	Southern Biotech
IgM	APC/BV421	G20-127	Mouse	IgG_1,κ	BD Bioscience
activated Caspase 3	FITC	C92-605	Rabbit	IgG	BD Bioscience
Ki-67	Ax700	B56	Mouse	IgG_1,κ	BD Bioscience
BCL-2	Pe	100	Mouse	IgG_1	Invitrogen
BCL-6	Pe	IG191E/A8	Mouse	IgG_1	Biolegend
IRF-4	eFluor660/FITC	3E4	Rat	IgG_1,κ	eBioscience
AID	FITC	Polyclonal	Rabbit	NA	Bioss
HLA-DR	Qdot800	Tu36	Mouse	IgG_2b	Invitrogen
Viability Dye	Aqua	NA	NA	NA	Invitrogen

[a] Green laser (532 mm) or yellow–green laser (561 nm) required.

with viremia, as viral loads at the time of necropsy were mostly undetectable (Fig. 1). Finally, the $CD21^+CD27^+$ resting memory B-cell sub-population in spleen cells of infected macaques was increased ($p=0.028$, Fig. 4E).

MZ B cell expression of co-stimulatory and activation markers in infected and uninfected macaques

We postulated that the declines in total B cells and MZ B cells in infected macaques might be driven by chronic activation. Therefore, we investigated co-stimulatory markers and markers of cell activation on splenic MZ B-cells. Expression of the co-stimulatory molecule CD86 (B7-2) was unaltered in splenic MZ B cells between healthy and chronically infected animals (Fig. 5A). In contrast, CD86 was significantly down-regulated in naïve, resting, and tissue-like memory B-cells of PBMC from the infected macaques ($p=0.0040$, 0.0040, and 0.028, respectively), with a similar tendency in activated memory ($CD21^-CD27^+$) cells (Fig. 5B). No difference was seen in expression levels of CD40 between healthy and chronically infected macaques. In both groups, over 95% of splenic MZ B-cells were positive (data not shown). On the other hand, CD69 expression was elevated in chronically infected animals compared to healthy (Fig. 5C) indicating low level activation, although the difference did not reach statistical significance. Splenic MZ B-cells from chronically infected animals similarly expressed higher levels of the proliferation marker Ki-67 with marginal significance ($p=0.048$, Fig. 5D) compared to the healthy controls. Other markers involved in control of B-cell activation and homeostasis such as CD272 (BTLA) and membrane bound Baff/BlyS (CD257) were expressed at slightly lower levels in the infected animals or remained unchanged (Fig. 5E and F). No difference in MHC-class II expression (HLA-DR) between healthy and chronically infected animals was observed (Fig. 5G).

In view of the higher Ki-67 expression on MZ B cells of infected macaques together with the suggestion of low-level activation, we investigated expression of caspase 3. In T-cells Caspase 3, an execution Caspase of the apoptosis pathway (MacKenzie and Clark, 2012), can be upregulated during activation (McComb et al., 2010). Further, HIV infection induces activation of Caspase 3 in human CD4 T-cells (Cicala et al., 2000). Whether similar up-regulation occurs in B cells is not known. Here, the expression of active Caspase-3 was slightly higher on MZ B cells of infected compared to uninfected macaques (Fig. 6A). In line with this result, expression of survival factor BCL-2 tended to be lower in SHIV infected animals (Fig. 6B). It is known that multiple caspases are able to cleave BCL-2 (Garcia-Saez, 2012; Guerrero et al., 2013). Although no significant changes were seen in splenic MZ B cells, we noted a significant drop in $CD40^+BCL\text{-}2^+$ expression in both activated and tissue like ($CD21^-CD27^-$) memory B-cell subsets in spleen and PBMC of infected macaques (Fig. 6C and D).

The drop in MZ B-cells post infection (Fig. 4D) was accompanied by a drop in IgD surface expression on splenic MZ B cells of infected macaques ($p=0.028$, Fig. 7A), together with a marginal increase in

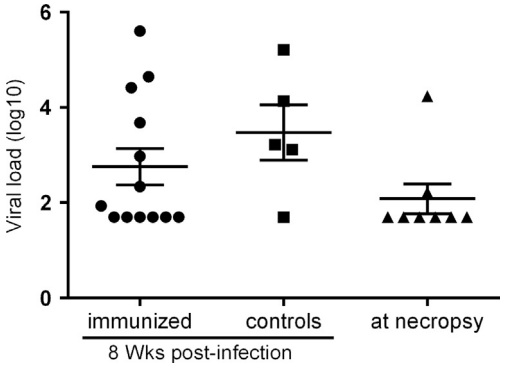

Fig. 1. Plasma viral loads in macaques at the time of sampling. LN were collected 8 weeks post-$SHIV_{SF162P4}$ infection from 13 previously immunized and 5 control macaques. Spleens and PBMC were collected from 8 $SHIV_{SF162P4}$-infected macaques at necropsy, (wk26–28 post challenge). Viremia for each macaque at the time of sample collection is shown with means and Standard error of the mean (SEM). The sensitivity of viral detection was 50 RNA copies/ml plasma.

Table 2
Characterization of marginal zone B-cells.

Marker	% Mean positive cells ranked highest to lowest
CD19	100[a]
CD20	100[a]
CD21	100[a]
CD38	> 95
CD272	> 95
CD40	> 95
CCR6	> 95
CD22	> 90
IgM	> 90
BCL-2	> 90
IgD	> 80
HLA-DR	> 80
CD95	~59
CD86	~35
CD257	~24
CD23	~10
CXCR4	< 10
CCR9	< 2
α4β7	< 2
Ki-67	< 1
CD69	< 1
BCL-6	< 0.5
active Caspase-3	< 0.1

[a] Essential marginal zone B-cell gating markers. MZ B-cells were evaluated in LN and spleen from healthy animals.

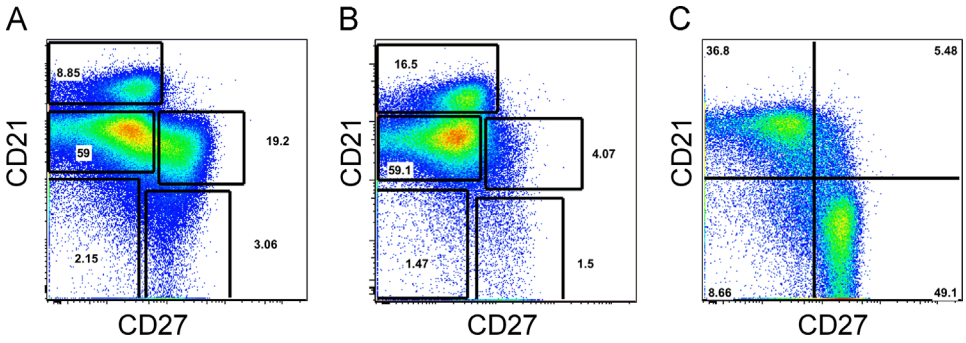

Fig. 2. Identification of MZ B-cells in rhesus macaque tissues. Representative flow cytometry staining of MZ B cells and memory B-cell sub-populations in spleen (A), LN (B) and PBMC (C). The MZ B-cell population stands out in spleen and LN as $CD21^{hi}$.

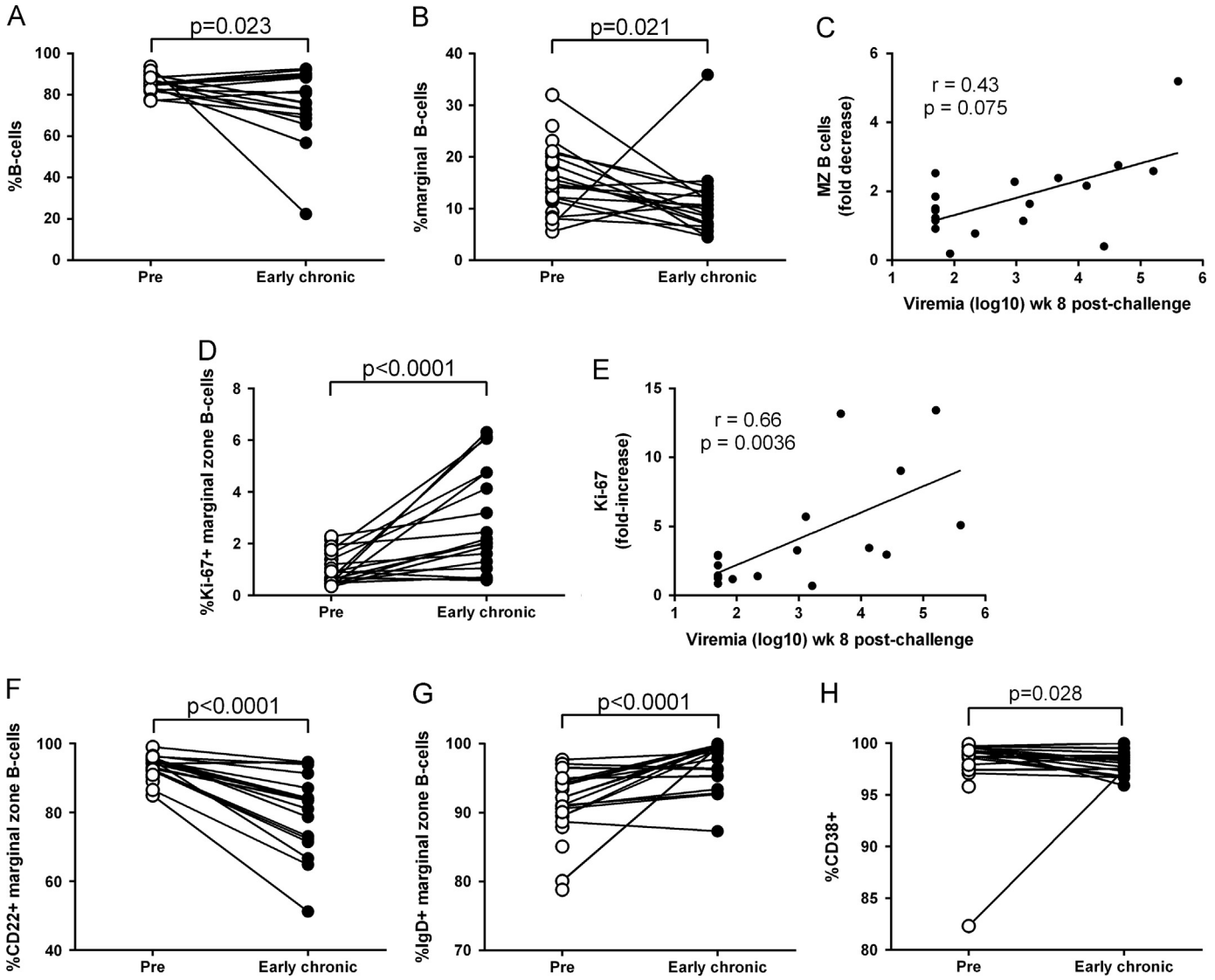

Fig. 3. Comparison of LN MZ B cells in healthy vs infected macaques in early chronic phase. Loss of total B-cells (A) and decrease in MZ B-cells 8 weeks post-infection (B) in axillary LN. Correlation of decrease in MZ B cells with viral load 8 weeks post-infection (C). Increase in Ki-67 expression on MZ B cells post-infection (D); mean difference 2.0% (95% C.I. 0.9% to 3.0%). Correlation of increase in Ki-67 expression with viral load 8 weeks post-infection (E). Comparison of CD22 (F); mean difference −13% (95% C.I. −8% to −19%), IgD (G); mean difference 5.5% (95% C.I. 3.4% to 7.5%), and CD38 (H) expression on MZ B cells pre- and post-infection; mean difference −0.5% (95% C.I. −1.5% to 0.3%). Linear regression lines shown on (C) and (E) are to aid interpretation of the data only (no functional form is implied).

$IgD^{-}IgM^{+}$ MZ B-cells ($p=0.048$, Fig. 7B). These findings corroborate the low-level activation and elevated expression of CD69 and Ki-67 in infected animals (Fig. 5C and D). Finally, we examined whether these changes were associated with altered homing properties of splenic MZ B-cells. The cells from chronically infected animals downregulated CCR6 expression ($p=0.028$, Fig. 7C). On the other hand, expression of CXCR4 and the mucosal homing marker α4β7 (Fig. 7D and E) on MZ B cells tended to increase in comparison to cells from healthy animals.

Differences between MZ B cells of healthy and infected macaques by PCR array

In late chronic infection, despite control of viremia to low or undetectable levels, low level chronic activation may have led to persistent differences between MZ B cells of healthy and infected animals. To further address this we sorted splenic MZ B-cells from 3 chronically infected and 3 healthy animals, isolated RNA, and compared expression levels of innate and adaptive response genes by Rhesus monkey specific PCR array. Using a stringent 2-fold increase or decrease in mean as well as median gene expression, we found substantial differences between the healthy and chronically infected animals (Table 3). The majority of down-regulated genes encoded cytokines and chemokines. Overall MZ B cells from infected animals were more limited in their capacity for producing cytokine/chemokines compared to healthy animals. On the other hand the majority of genes that were upregulated in infected compared to uninfected macaques were transcription factors including IRF-1, FoxP3, T-box 21 and signaling molecules NLRP3, STAT1 (Table 3). Interestingly chemokine receptors CXCR3 and CCR5 were elevated in infected monkeys, indicating some changes in homing pattern as observed for α4β7 and CXCR4. Not only did MZ B cells from infected macaques downregulate chemokines and cytokines, corresponding receptors were downregulated too, further indicating that the cells are limited in the ability to respond to outside stimuli (Table 3). In line with this, down-regulation of innate receptors TLR3 and TLR5 was also observed.

Discussion

There is good agreement on the definition of splenic MZ B cells of mouse and human as $CD21^{+/hi}$, IgM^{hi}, IgD^{lo}, and $CD23^{-/lo}$

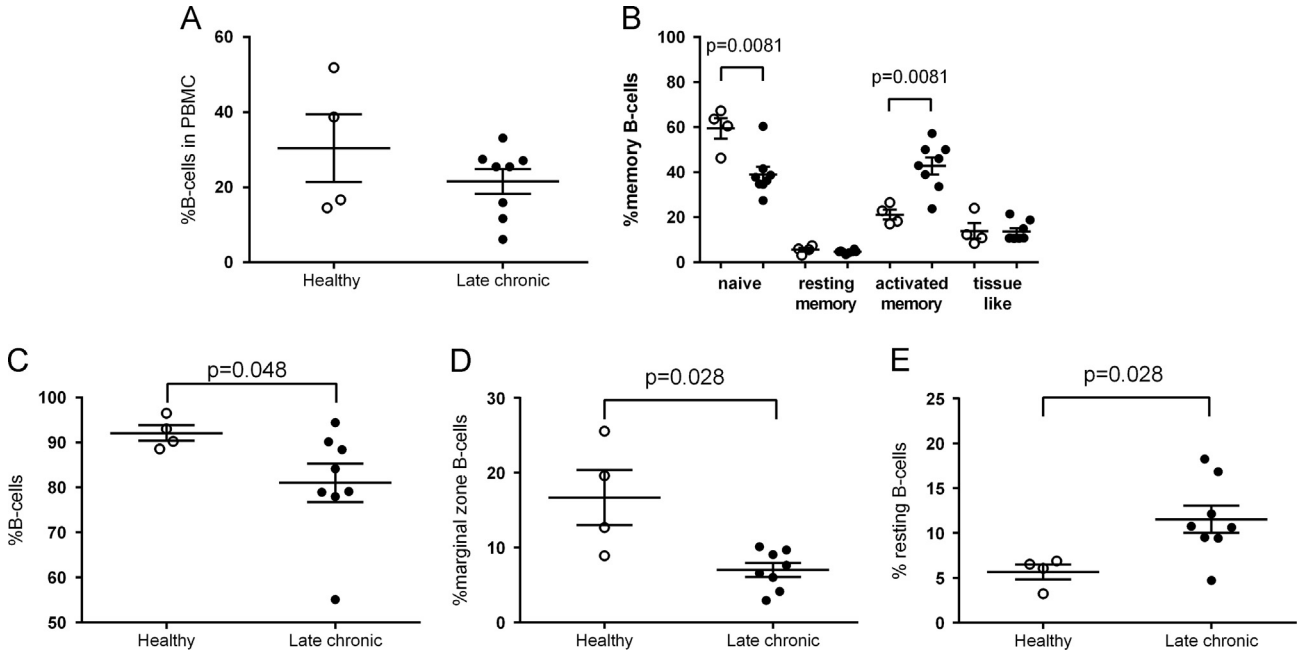

Fig. 4. Comparison of splenic B cells in healthy vs infected macaques in late chronic phase. No difference in total B-cell frequency in PBMC (A), but skewing of memory B-cell populations in PBMC (B) following $SHIV_{SF162P4}$ infection (infected, closed circles; uninfected, open circles). Differences in total B-cells (C), MZ B-cells (D) and resting B-cells (E) in spleen between infected and healthy animals. Error bar=SEM.

(Martin and Kearney, 2002; Weill et al., 2009; Cerutti et al., 2013). Additional markers have been reported, including $CD1^{hi}$ (Martin and Kearney, 2002), $CD1c^{+}$ and $CD27^{+}$ (Weill et al., 2009; Cerutti et al., 2013), and $CD5^{-}$ (Weill et al., 2009). Human MZ B cells have also been described as $CD10^{-}$ (Chagnon-Choquet et al., 2014). Not many publications have addressed MZ B-cells in non-human primates although B cell memory subpopulations have been examined in secondary lymphoid tissues (Das et al., 2011; Demberg et al., 2012; Titanji et al., 2010). Vugmeyster et al. (2004) identified CD21 as a marker of cynomolgus monkey MZ B cells, consistent with the MZ B cell phenotype of mice and humans. Here we confirm the $CD21^{hi}$ phenotype of rhesus macaque MZ B cells (Fig. 2A). While we did not stain for CD1, CD1c, CD10 or CD5, we confirmed low expression of CD23 and high expression of CD22 (Fig. 3F and Table 2). We observed high expression of IgM on rhesus MZ B-cells (Table 2); the majority of cells co-expressed IgD (data not shown). While CD27 is expressed on human MZ B cells at relatively high levels (Weill et al., 2009; Chagnon-Choquet et al., 2014), our data categorizing rhesus macaque MZ B-cells as $CD27^{-/dim}$ are in line with Vugmeyster et al., (2004) who described cynomolgus monkey MZ B cells as $CD27^{-/+}$, and in contrast to results of Peruchon et al. (2009) who described cynomolgus monkey MZ B cells as $CD27^{+}IgD^{+}$. We were unable to detect $CD21^{hi}$ B-cells in blood (data not shown), which might be in part due to the extremely low frequency of $CD21^{hi}$ compared to $CD27^{+}IgD^{+}$ cells in Rhesus macaques. A similar observation was also reported by Vugmeyster et al. (2004) for cynomolgus monkeys. While Messaoudi et al. (2011) described MZ-like cells in blood of rhesus macaques, the CD21 marker was not used. The lack of circulating $CD21^{hi}$ MZ B-cells could point to a species difference between humans and non-human primates. Overall our data with regard to the frequency of MZ B-cells in axillary LN (~16%) and spleen (~17%) are in accord with results of Peruchon et al. (2009) (LN, ~22% and spleen, ~17%) and higher compared to Vugmeyster et al. (2004).

We report here high level expression of CD38 on rhesus macaque MZ B cells (Table 2, Fig. 3H), consistent with similar high expression on mouse MZ B cells (Oliver et al., 1997; Pillai et al., 2005). Reports on human cells have been conflicting, and require further clarification. Colombo et al. (2013) reported human splenic MZ B-cells to be $CD38^{-}$ while Benitez et al. (2014) by gating on CD24 and CD38 identified a B-cell population in human spleen characteristic of MZ B-cells that was $CD38^{+}$ $CD21^{hi}$. MZ B-cells play a role in the early immune response to pathogens in a T-independent and T-dependent fashion (Zouali and Richard, 2011). CD38 has been shown to be important for the innate response to *Listeria* infection (Lischke et al., 2013). Further, in bulk purified mouse spleen B-cells stimulated with TLR7 agonist, anti-CD38 antibody and IL-4 led to a strong increase in production of IgM and to a varying degree also induced IgG1 production (Tsukamoto et al., 2009). Thus expression of CD38 on MZ B-cells as shown here would be meaningful for mounting rapid responses triggered through innate receptors.

CD22 was highly expressed on rhesus macaque MZ B-cells in both spleen (data not shown) and LN (Fig. 3F), similar to the high expression reported for mouse and human MZ B-cells (Martin and Kearney, 2002; Colombo et al., 2013). CD22 is a negative regulator of B-cell activation (Muller and Nitschke, 2014), and in mice B-cell homeostasis requires CD22 and BlyS (BAFF)-BR3 signaling for survival (Smith et al., 2010). MZ B-cells were shown to be reduced using anti-Baff and anti-CD22 antibodies (Smith et al., 2010). Similarly, a Baff antagonist decreased MZ B cells in cynomolgus monkeys (Vugmeyster et al., 2006). Here we showed that over 20% of splenic MZ B-cells were positive for membrane bound Baff/BlyS (Fig. 5E). There was no difference in Baff expression between SHIV-infected and healthy animals, consistent with a previous report showing no difference in plasma Baff levels between HIV infected children and healthy controls (Cagigi et al., 2010).

In mice MZ B-cells express high levels of MHC class II, CD80 and CD86 (Cerutti et al., 2013). Our findings for rhesus macaque MZ B-cells show some similarities. The majority of splenic $CD21^{hi}$ MZ B-cells were positive for MHC-class II (Table 2). We did not investigate CD80, but CD86 was moderately expressed (Fig. 5A, Table 2). Mouse MZ B-cells express high levels of CD40 (Oliver et al., 1997). We found high expression of CD40 on Rhesus MZ B-cells (Table 2) consistent with the mouse data.

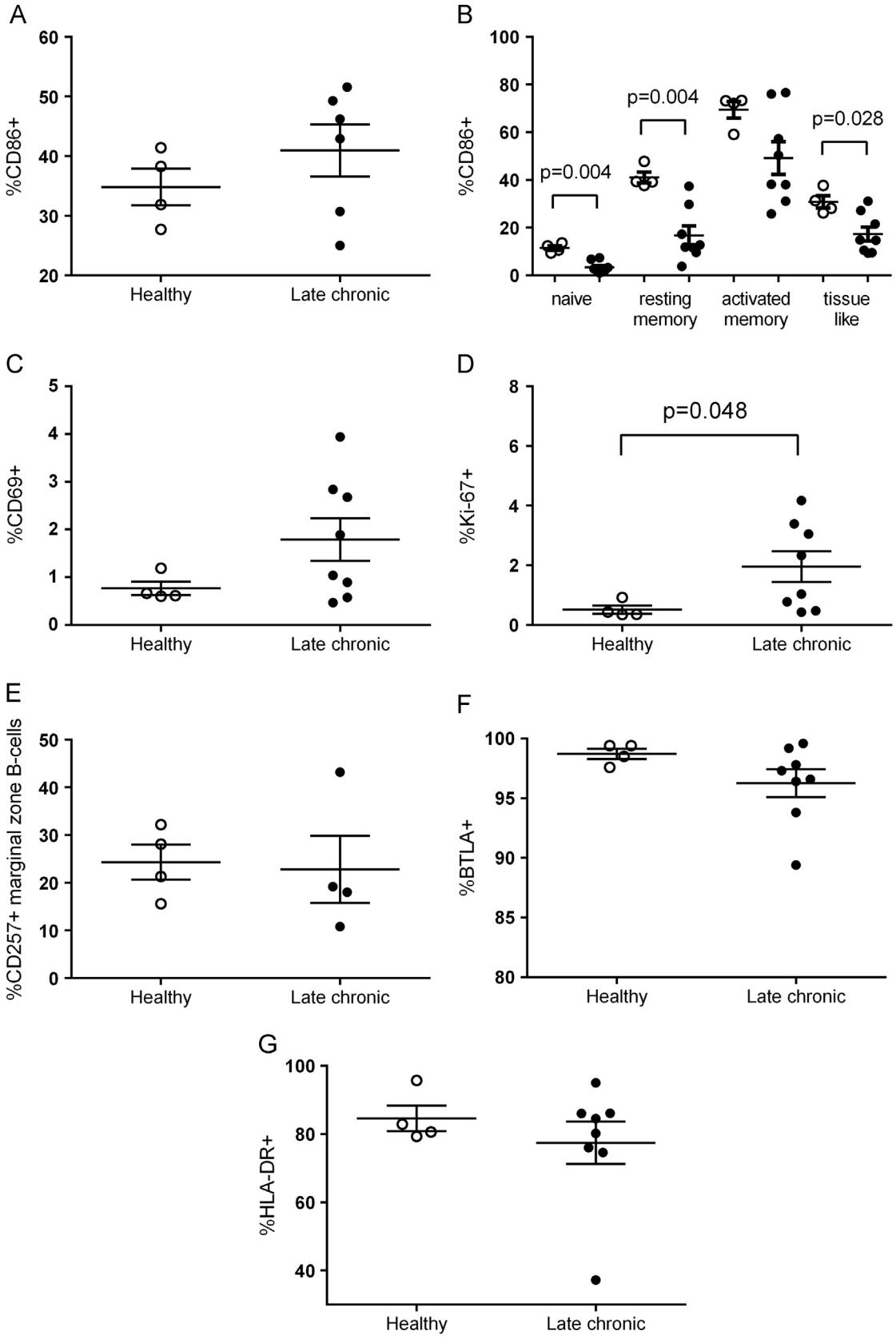

Fig. 5. Differential expression of activation markers on MZ B-cells in spleen between infected and healthy animals. Expression of activation marker CD86 on splenic MZ B-cells of infected and uninfected animals (A); and on memory B-cell populations in PBMC of infected (closed circles) and uninfected (open circles) macaques (B). Expression of the activation marker CD69 (C) and the proliferation marker Ki-67 (D) on MZ B-cells of infected and uninfected animals. Expression of MZ B-cell bound Baff (CD257) (E), the negative regulatory receptor BTLA (CD272) (F), and HLA-DR (G) on MZ B cells of infected and uninfected animals. Error bar = SEM.

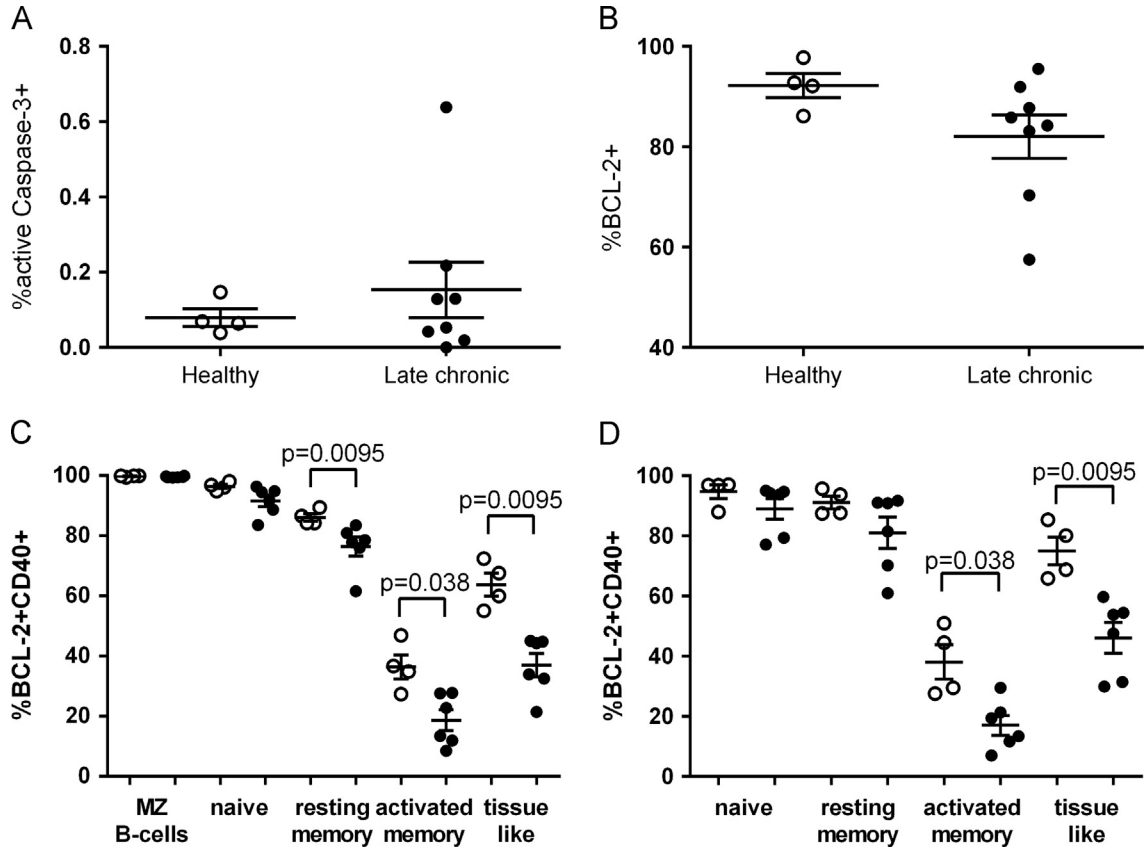

Fig. 6. Comparison of apoptosis and survival marker expression by splenic MZ B-cells between healthy and SHIV infected animals. Trends for elevation of active Caspase 3 expression (A) and decreased BCL-2 expression (B) on MZ B-cells from infected animals. Changes in co-expression of BCL-2 and CD40 in memory B-cell sub-populations of spleen (C) and PBMC (D) between infected (closed circles) and healthy (open circles) animals were observed. Error bar=SEM.

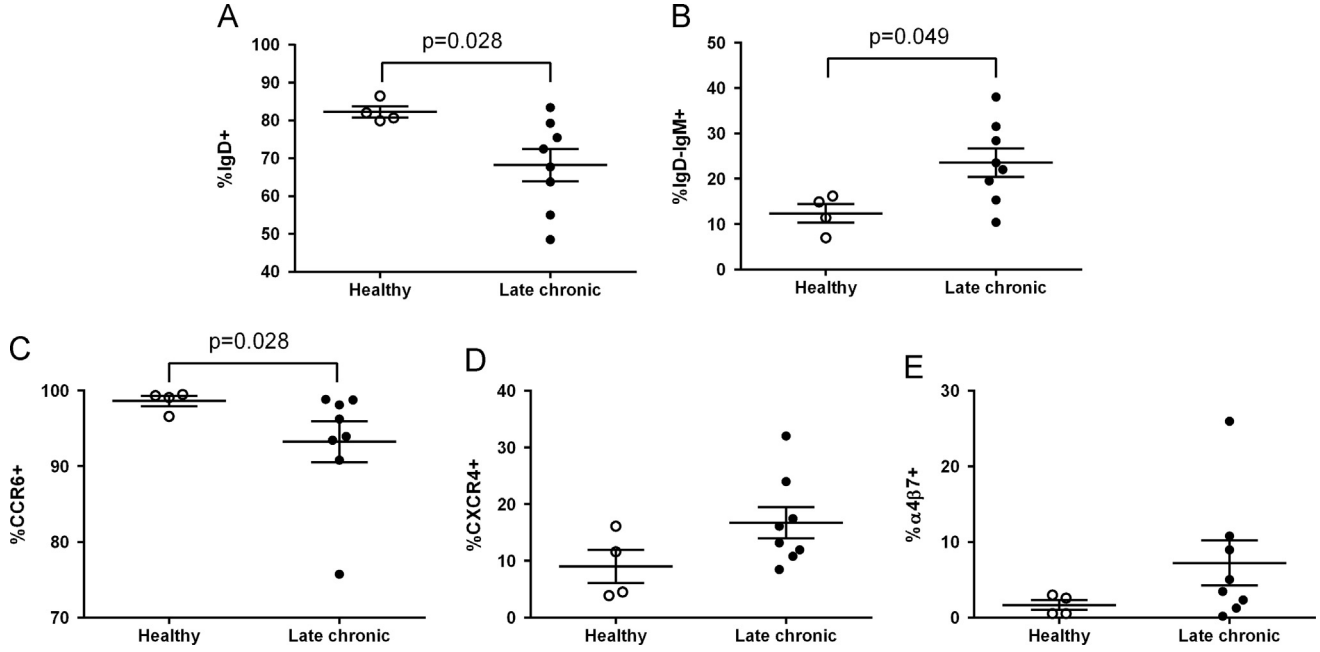

Fig. 7. Changes in isotype and homing marker expression on splenic MZ B-cells between infected and healthy animals. MZ B-cells from infected animals down regulated the expression of IgD (A) while the frequency of $IgD^{-}IgM^{+}$ MZ B-cells increased (B). Homing receptor CCR6 expression was significantly lower (C), while CXCR4 (D) and α4β7 (E) expression levels were elevated on MZ B-cells of infected animals. Error bar=SEM.

The B and T lymphocyte attenuator (BTLA, CD272), a lymphocyte inhibitory receptor with similarities to CTLA-4 and PD-1 on T cells (Watanabe et al., 2003) was highly expressed on $CD21^{hi}$ splenic MZ B cells (Table 2, Fig. 5F). This is consistent with the high expression of BTLA on unstimulated $IgD^{+}CD27^{+}$ B-cells in the blood of healthy volunteers (Thibult et al., 2013). These cells are considered to be MZ-like B-cells (Messaoudi et al., 2011; Peruchon et al., 2009). In humans, B-cell activation via TLR9 (CPG-ODN DNA)

Table 3
Differences in RNA expression of SHIV-infected versus healthy rhesus macaques by PCR array analysis.

UniGene		Fold Decrease (Mean)	Fold Decrease (Median)	Fold Increase (Mean)	Fold Increase (Median)
	Cytokines/chemokines				
Mmu.3376	IL-6	.	2.1	.	.
Mmu.3491	CCL2	7.1	22.0	.	.
Mmu.3665	CSF2	9.0	36.0	.	.
Mmu.15664	IFN-b1	4.4	11.0	.	.
Mmu.3374	IL-10	6.3	8.9	.	.
Mmu.3675	IL-13	12.4	27.7	.	.
Mmu.3414	IL-15	2.3	2.3	.	.
Mmu.14785	IL-17A	7.9	22.2	.	.
Mmu.3361	IL-1a	11.1	25.5	.	.
Mmu.3415	IL-2	5.4	16.8	.	.
Mmu.18854	IL-23A	2.7	2.7	.	.
Mmu.3375	IL-4	7.3	23.3	.	.
Mmu.3363	IL-8	7.0	16.1	.	.
Mmu.3698	CCL5	.	.	2.1	.
	Cytokine/chemokine receptors				
Mmu.12735	IL-1R1	5.0	7.7	.	.
Mmu.14927	CCR4	4.0	10.9	.	.
XM_001084047	CCR8	6.0	12.7	.	.
Mmu.8534	CXCR3	.	.	2.3	.
Mmu.3440	CCR5	.	.	2.2	2.2
	Complement components				
Mmu.3133	C3	2.8	2.8	.	.
Mmu.3027	LBP	11.2	37.8	.	.
Mmu.3409	MBL2	18.2	59.3	.	.
	PRR/inflammasome				
Mmu.12334	NLRP3	.	.	.	2.2
Mmu.3813	TLR3	2.3	4.2	.	.
Mmu.3815	TLR5	3.9	6.6	.	.
	Signaling/transcription				
Mmu.13224	STAT4	.	3.0	.	.
Mmu.13939	T-box 21	.	.	.	2.2
Mmu.11578	IRF-1	.	.	3.0	2.7
Mmu.3514	STAT1	.	.	2.7	2.8
Mmu.3791	FOXP3	.	.	2.9	2.7
Mmu.13081	IRF-6	3.0	3.2	.	.
XM_001084631	RAG1	11.1	30.1	.	.
	Co-stimulatory				
Mmu.3359	CD80	.	.	.	2.1
	Acute phase/anti-bacterial				
Mmu.3013	CRP	12.1	36.3	.	.
XM_001103896	MPO	8.8	20.5	.	.
Mmu.1820	Lysozyme	.	.	3.7	4.4
	Others				
Mmu.11930	Serum amyloid P component	6.1	6.8	.	.
Mmu.12026	Solute carrier fam. 11	2.4	2.3	.	.

Spleen derived marginal zone B-cells were sorted as described in Materials and methods section ($n=3$ healthy vs $n=3$ infected). The different analytical methods comparing the mean or median fold up- or down-regulation delivered similar results. PRR=Pattern Recognition Receptors.

induced and sustained expression of BTLA (Thibult et al., 2013). This observation is of interest as TLR9 signaling drives human transitional ($CD24^{hi}$) B-cells towards the MZ B-cell pathway (Guerrier et al., 2012). The role of BTLA receptor on MZ B-cells is unclear, but it might help regulate T-cell independent immunoglobulin production (Thibult et al., 2013).

Literature on expression of homing markers on MZ B-cells is somewhat scarce. However CCR6 expression in human spleen samples was specifically seen in mantle and marginal zones but not in follicles (Rodig et al., 2002), suggesting that MZ B-cells might be CCR6 positive. Further, 84% of marginal zone/MALT lymphomas tested positive for the expression of CCR6 in contrast to no follicular lymphomas (Rodig et al., 2002). Our flow data confirm that CCR6 is highly expressed on Rhesus MZ B-cells (Table 2, Fig. 7C). Low level expression of CXCR4 and $\alpha4\beta7$ was also observed (Fig. 7D and E).

Having extensively phenotyped rhesus macaque MZ B cells, we compared features of this B cell population in early and late chronic $SHIV_{SF162P4}$ infection to uninfected animals. Cynomolgus monkeys display a decline in MZ B cells within the first 4 weeks of SIV infection (Peruchon et al., 2009). Our LN data during early chronic phase, wk8 post-infection, showed a similar decrease, which persisted in splenic MZ B cells in late chronic phase. This overall decline might be attributable to differentiation of these cells into antibody secreting cells which lose the $CD21^{hi}$ phenotype as described by Zouali and Richard (Zouali and Richard, 2011). We confirmed in preliminary experiments using *ex-vivo* TLR ligand stimulation of rhesus macaque splenic B cells that $CD21^{hi}$ cells are lost 3 days post-stimulation (unpublished). Thus the decline in MZ B-cells might be attributable to cell differentiation into other phenotypes.

Not only are MZ B cells reduced in LN and spleen in early (Fig. 4B) and chronic SHIV infection (Fig. 4D), but also total B-cells are reduced (Fig. 3A; Fig. 4C). We considered that dysregulation of CD40L, provided by CD4 T cells, might have contributed to these reductions. In the absence of CD40L, B-cells might become anergic and undergo apoptosis, as it is known that activation by CD40 cross-linking induces strong proliferative responses in MZ B cells (Oliver et al., 1997). However, CD40L can also be expressed on DC during viral infections,

resulting from TLR stimulations (Johnson et al., 2009). Therefore a CD40L signal could be provided by DC or related cells of the monocyte/macrophage lineage present in the marginal zone Gordon et al., 2014. In any case, the question regarding CD40L provided by CD4 T cells is moot, as no decline in this cell population was observed over the course of infection, at least in peripheral blood. Absolute CD4 T cell counts prior to challenge and 8 and 20 weeks post-challenge were 834 ± 81, 821 ± 76, and 800 ± 84 for the vaccinated macaques and 808 ± 92, 755 ± 78, and 844 ± 129 for the control macaques, respectively. We did not evaluate CD4 T cell counts in LN and spleen.

It has been well documented that skewing of B-cell memory populations occurs following SIV/SHIV infection, and our data confirm this (Fig. 4B). The inhibitory molecules CD22 and BTLA were expressed at lower levels in SHIV infection, CD22 significantly so (Fig. 3F). In contrast to the downregulation seen here, upregulation of CD22 has been described as a feature of an exhausted B-cell phenotype among different human B-cell populations (Moir and Fauci, 2009; Moir et al., 2008). The conflicting results might represent species differences.

We observed changes in homing markers, noting a skewing following SHIV infection, with significantly lower expression of CCR6 on splenic MZ B-cells obtained in the late chronic phase (Fig. 7C). Trends towards increases in the expression of CXCR4 (Fig. 7D) and α4β7 (Fig. 7E) were also observed. CXCR4 is important for shuttling between light and dark zones of germinal centers (Allen et al., 2007; Victora and Mesin, 2014). However, whether MZ B-cells, potentially laden with antigen post-infection increase trafficking to the light zone to present captured antigen to other B-cells or follicular dendritic cells remains speculation at this point. The non-significant increases in α4β7 and CXCR4 expression (Fig. 7D and E) might also suggest that some MZ B-cells having acquired an "activated" phenotype marked by Ki-67 and CD69 upregulation (Fig. 5C and D) are prepared for homing to the mucosa (α4β7) or bone marrow (CXCR4).

Trends toward decreased BCL-2 and increased active Caspase 3 expression in splenic MZ B cells late in the chronic phase of SHIV infection (Fig. 6A and B) were associated with increased $CD69^+$, $Ki\text{-}67^+$, and IgM^+ cells. CD69 is a common T-cell activation marker, but its regulation differs in B-cells (Vazquez et al., 2009) where Toll-like receptor as well as BCR engagement can increase its expression (Minguet et al., 2008). While TLR stimulation leads to upregulation of CD40 as well as CD69 (Jain et al., 2011; Kaminski et al., 2012), we did not observe higher levels of CD40 on MZ B-cells in infected animals (Fig. 6C and data not shown). However, CD40 already exhibited high baseline expression levels (Table 2). Overall, our findings here support the hypothesis that the marginal zone B-cells are "lost" in part due to constant immune activation. Future work will be needed to substantiate this hypothesis.

The PCR array data obtained from a limited number of animals must be interpreted cautiously but raises interesting questions for future exploration. Using a stringent 2-fold cut off, we observed that many cytokines/chemokines that can be produced by B cells, such as GM-CSF, IFN-b1, IL-10, IL-13, IL-1a, IL-2, IL-4 and IL-8 (Hamze et al., 2013; Pistoia, 1997) were downregulated (Table 3). Whether MZ B-cells can produce and secrete all of the cytokine/chemokines we detected by RNA needs further verification. While IL-10 secretion has been attributed to MZ B-cells, for example (Buchta and Bishop, 2014; Shen et al., 2013), RNA (cDNA) detection does not necessarily relate to translated protein as shown for IL-15 (Onu et al., 1997). The downregulation of complement component C3, but upregulation of MBL2 might indicate skewing of the complement system's physiological roles beyond the scope of host defense as discussed by Kolev et al. (2014). Whether MZ B cells play a role in the complement mediated crosstalk between cell effector systems warrants further research. The TNF-family death receptor CD95 (FAS) was slightly elevated (1.6-fold) in chronic infection although it did not reach the 2-fold cut-off. Thus we cannot rule out that the loss of some MZ B-cells might be due to FAS-FAS-L mediated apoptosis. On the other hand FAS has also shown non-apoptotic activities such as cellular activation, proliferation and maturation, as discussed elsewhere (Peter et al., 2007; Strasser et al., 2009), and therefore may not have contributed to MZ B cell loss. Expression of TLRs on Rhesus macaque B-cells has not been described, but it might be similar to that of humans. TLRs are expressed to varying degrees on human B-cell subsets (Buchta and Bishop, 2014; Dorner et al., 2009). In mice, TLR3 seems to be somewhat more broadly expressed on MZ B-cells (Buchta and Bishop, 2014). However, the contributions of TLR signaling to the development and function of human MZ B-cells have not been elucidated (Weill et al., 2009). We observed a non-significant decline in the expression of TLR5 and also TLR3 on MZ B cells from infected animals. This loss of TLR expression could be in line with activation induced differentiation into another B-cell phenotype, as discussed above. Tonsilar memory B-cells in humans do not express TLR3 and express reduced levels of TLR5 (Dorner et al., 2009). However whether a MZ B-cell can differentiate into a B-cell memory phenotype, for example, needs to be further investigated.

In summary we have confirmed the MZ B cell phenotype previously described for cynomolgus monkeys and extended the phenotype of this B cell subpopulation to spleen and LN tissues of rhesus macaques. In addition we show that SHIV affects MZ B-cells early in chronic infection, and that these effects persist in late chronic phase despite control of plasma viremia to low or undetectable levels. Thus we extend the work of Peruchon et al. (2009) who showed alteration in the MZ B cell population of cynomolgus monkeys during the first four weeks of SIV infection. Effects of long-term SHIV infection shown here included changes in frequency, activation, regulatory markers, antibody isotypes and homing preferences. The changes observed suggest that the ability of MZ B cells to fulfill their role as mediators of early adaptive immune responses is hampered by virus infection. At this moment it is unknown if the loss of MZ-B-cells is unique to SHIV infection or is a more common occurrence in chronic viral infections. Unpublished work by Stephen Waggoner and Stacey Cranert (Cincinnati Children's Hospital Medical Center; personal communication), shows that MZ B-cells are also lost in chronic LCMV infection of mice. Further, both a loss and an increase of MZ B-cells was reported following infection of mice with two different species of Borrelia Malkiel et al., (2009). Thus the pathogen might play an important role in the biology of MZ B-cells. *Ex-vivo* stimulation experiments from sorted MZ B-cells are needed to further elucidate the role and functions of this subset in the SHIV and SIV Rhesus macaque models. Overall, loss or dysregulation of MZ B-cells could impact antibody responses to the ongoing infection, acquisition of opportunistic infections, as well as HIV therapeutic vaccine approaches.

Materials and methods

Macaque samples

Animals were housed at Advanced BioScience Laboratories, Inc. (ABL; Rockville, MD) or at the NCI Animal Facility (Bethesda, MD), and maintained in accordance with the standards of the American Association for Accreditation of Laboratory Animal Care and the NIH Guide for the Care and Use of Laboratory Animals. Experimental protocols were reviewed and approved by Institutional Animal Care and Use Committees prior to initiation of studies. Lymph node (LN) samples were obtained retrospectively from a previously published pre-clinical rhesus macaque vaccine study (Thomas et al., 2014) pre-vaccination ($n=24$, 16 immunized and 8 controls) and at the initiation of the chronic phase of infection,

8 weeks after intrarectal $SHIV_{SF162P4}$ challenge ($n=18$, 13 immunized and 5 controls). At this time point, plasma viral loads between immunized and control macaques were not different (Fig. 1), so the LNs were grouped for further study. In addition, spleens and PBMC were obtained from a random subset of animals ($n=8$) from that study at necropsy in late chronic phase (26 to 28 weeks post-infection) at which time viral loads were undetectable in 6 of the 8 macaques (Fig. 1). Geometric mean viral loads for the macaques studied at wk 8 post-infection and at necropsy were 9.0×10^2 and 1.2×10^2 RNA copies/ml plasma, respectively. Spleens from 4 uninfected animals were used as controls.

Tissue preparation

PBMC were isolated by ficoll paque (GE Healthcare) gradient centrifugation, washed and remaining red blood cells were lysed with ACK lysis buffer (Lonza). Splenocytes and LN cells were isolated by cutting the spleen or LN open and carefully scraping out the cells. The isolated cells were mixed with culture medium and passed through a 70 μm cell strainer (BD biosciences). After washing, red blood cells were lysed using ACK lysis buffer. Following a subsequent wash in PBS the cells were counted and used fresh for flow cytometry staining. Remaining cells were viably frozen and stored in liquid nitrogen until further use.

Flow cytometry

For cellular phenotyping $1–2\times10^6$ cells/tube were used per staining. Antibody details are summarized in Table 1. In brief, following 25 min surface staining, cells were washed in PBS, fixed and permeabilized according to the manufacturer's instructions using Fix and Perm or a transcription buffer set for IRF-4 and BCL-6 (BD Bioscience, San Jose, CA). After washing, intracellular staining was conducted according to the respective buffer set instructions. After staining, cells were washed, resuspended in PBS containing 2% Formaldehyde (Tusimis, Rockville, MD), and acquired within 24 h on a custom 4-laser LSR II (BD Bioscience). A minimum of 50000 live cells in the lymphocytic gate were acquired in DIVA. Analysis was performed in FlowJo, and data were exported into Excel and GraphPad Prism 6.

For the sorting of spleen cells from healthy and randomly chosen SHIV-infected macaques, approximately 20×10^6 viable cells were stained per sample. Cells were thawed and washed in RPMI1640 with L-glutamine and anti-bacterial anti-fungal solution (all from Invitrogen). The cells were counted and stained with viability dye aqua followed by surface staining with CD2 PE, CD14 Qdot605, CD19 PeCy5, CD21 PeCy7 and CD27 PerCP-eF710. Dead cells, $CD2^+$ and $CD14^+$ cells were excluded, and MZ B-cells were sorted as $CD19^+$ and $CD21^{bright}$ on the highest purity setting using a 75-um nozzle on a FACSAria II (BD Bioscience) or a MoFlo Astrios EQ (Beckman Coulter).

Rhesus macaque PCR array

RNA from sorted cells was extracted using the Qiagen RNeasy mini kit. cDNA was generated after quantifying RNA yield and purity on a Nanodrop photometer with the Qiagen QuantiTect reverse transcription kit with genomic DNA elimination buffer. PCR array plates (RT^2 Profiler PCR array no. 330231PAQQ-052ZA, Qiagen) were handled and loaded according to the manufacturer's instructions. For the PCR reaction we used Invitrogen SYBR greenER PCR universal mix and an ABI 7500 real-time PCR machine. Data were analyzed using SDS software, exported into Excel and GraphPad Prism. Differences were calculated with the ΔΔCt method and undetectable responses were set to a Ct value of 35 (cut-off value for positive signal) to allow for comparison and statistical analysis. An increase or decrease of 2-fold was used as a cut-off criterion.

Statistical analysis

The comparisons between healthy controls ($n=4$) and infected animals ($n=8$) over several classes of outcomes were assessed using the exact Wilcoxon rank sum test. Changes from pre-infection to week 8 post-infection in total B-cells, MZ B-cells and the expression of Ki-67, CD22 and IgD were modeled using repeated measures analysis of variance after logarithmic transformation of the raw data. Correlations of MZ B-cell and Ki-67 changes with viral loads were calculated by the Spearman method. For the paired analyses of CD27 and CD38 MFIs in B-cell subsets, the exact Wilcoxon signed rank test was used. Due to the exploratory nature of this investigation, p values were not corrected for multiple comparisons. Values <0.05 therefore indicate noteworthy differences and were labeled as significant, but some conclusions involving simultaneous tests or values >0.01 are tentative until confirmed in independent studies. Informal consideration was given to the internal consistency of potentially correlated results and to the limited power of nonparametric methods applied to data from the small numbers of available animals in this study.

Acknowledgments

We thank D.J. Liewehr for helping with the statistical analysis, critical reading of the manuscript and helpful suggestions. We further thank S. Waggoner and S. Cranert, Cincinnati Children's Hospital Medical Center, for sharing some of their unpublished LCMV work with us. This work was supported by the Intramural Research Program of the National Institutes of Health, National Cancer Institute.

References

Allen, C.D., Okada, T., Cyster, J.G., 2007. Germinal-center organization and cellular dynamics. Immunity 27, 190–202.

Benitez, A., Weldon, A.J., Tatosyan, L., Velkuru, V., Lee, S., Milford, T.A., Francis, O.L., Hsu, S., Nazeri, K., Casiano, C.M., Schneider, R., Gonzalez, J., Su, R.J., Baez, I., Colburn, K., Moldovan, I., Payne, K.J., 2014. Differences in mouse and human nonmemory B cell pools. J. Immunol. 192, 4610–4619.

Buchta, C.M., Bishop, G.A., 2014. Toll-like receptors and B cells: functions and mechanisms. Immunol. Lett. 59, 12–22.

Cagigi, A., Palma, P., Nilsson, A., Di Cesare, S., Pensieroso, S., Kakoulidou, M., Bernardi, S., Rossi, P., Chiodi, F., 2010. The impact of active HIV-1 replication on the physiological age-related decline of immature-transitional B-cells in HIV-1 infected children. Aids 24, 2075–2080.

Carroll, M.C., Isenman, D.E., 2012. Regulation of humoral immunity by complement. Immunity 37, 199–207.

Cerutti, A., Cols, M., Puga, I., 2013. Marginal zone B cells: virtues of innate-like antibody-producing lymphocytes. Nat. Rev. Immunol. 13, 118–132.

Chagnon-Choquet, J., Fontaine, J., Poudrier, J., Roger, M., Montreal, Primary, H.I.V.I.S. G., Slow Progressor Study, G, 2014. IL-10 and lymphotoxin-alpha expression profiles within marginal zone-like B-cell populations are associated with control of HIV-1 disease progression. PLoS One 9, e101949.

Cicala, C., Arthos, J., Rubbert, A., Selig, S., Wildt, K., Cohen, O.J., Fauci, A.S., 2000. HIV-1 envelope induces activation of caspase-3 and cleavage of focal adhesion kinase in primary human CD4(+) T cells. Proc. Natl. Acad. Sci. U.S.A. 97, 1178–1183.

Colombo, M., Cutrona, G., Reverberi, D., Bruno, S., Ghiotto, F., Tenca, C., Stamatopoulos, K., Hadzidimitriou, A., Ceccarelli, J., Salvi, S., Boccardo, S., Calevo, M.G., De Santanna, A., Truini, M., Fais, F., Ferrarini, M., 2013. Expression of Ig receptors with distinctive features indicating antigen selection by marginal zone B cells from human spleen. Mol. Med..

D'Orsogna, L.J., Krueger, R.G., McKinnon, E.J., French, M.A., 2007. Circulating memory B-cell subpopulations are affected differently by HIV infection and antiretroviral therapy. Aids 21, 1747–1752.

Das, A., Veazey, R.S., Wang, X., Lackner, A.A., Xu, H., Pahar, B., 2011. Simian immunodeficiency virus infection in rhesus macaques induces selective tissue specific B cell defects in double positive CD21+CD27+ memory B cells. Clin. Immunol. 140, 223–228.

Demberg, T., Brocca-Cofano, E., Xiao, P., Venzon, D., Vargas-Inchaustegui, D., Lee, E. M., Kalisz, I., Kalyanaraman, V.S., Dipasquale, J., McKinnon, K., Robert-Guroff, M, 2012. Dynamics of memory B-cell populations in blood, lymph nodes, and bone marrow during antiretroviral therapy and envelope boosting in simian

immunodeficiency virus SIVmac251-infected rhesus macaques. J. Virol. 86, 12591–12604.
Dorner, M., Brandt, S., Tinguely, M., Zucol, F., Bourquin, J.P., Zauner, L., Berger, C., Bernasconi, M., Speck, R.F., Nadal, D., 2009. Plasma cell toll-like receptor (TLR) expression differs from that of B cells, and plasma cell TLR triggering enhances immunoglobulin production. Immunology 128, 573–579.
Garcia-Saez, A.J., 2012. The secrets of the Bcl-2 family. Cell Death Differ. 19, 1733–1740.
Gordon, S., Phuddemann, A., Mukhopadhyay, S., 2014. Sinusoidal immunty: macrophages at the lymphohematopoietic interface. Cold Spring Harbor Perspect. Biol. 7, a016378.
Guerrero, A.D., Welschhans, R.L., Chen, M., Wang, J., 2013. Cleavage of anti-apoptotic Bcl-2 family members after TCR stimulation contributes to the decision between T cell activation and apoptosis. J. Immunol. 190, 168–173.
Guerrier, T., Youinou, P., Pers, J.O., Jamin, C., 2012. TLR9 drives the development of transitional B cells towards the marginal zone pathway and promotes auto-immunity. J. Autoimmun. 39, 173–179.
Hamze, M., Desmetz, C., Guglielmi, P., 2013. B cell-derived cytokines in disease. Eur. Cytokine Netw. 24, 20–26.
Ho, J., Moir, S., Kulik, L., Malaspina, A., Donoghue, E.T., Miller, N.J., Wang, W., Chun, T.W., Fauci, A.S., Holers, V.M., 2007. Role for CD21 in the establishment of an extracellular HIV reservoir in lymphoid tissues. J. Immunol. 178, 6968–6974.
Jain, S., Chodisetti, S.B., Agrewala, J.N., 2011. CD40 signaling synergizes with TLR-2 in the BCR independent activation of resting B cells. PLoS One 6, e20651.
Johnson, S., Zhan, Y., Sutherland, R.M., Mount, A.M., Bedoui, S., Brady, J.L., Carrington, E.M., Brown, L.E., Belz, G.T., Heath, W.R., Lew, A.M., 2009. Selected Toll-like receptor ligands and viruses promote helper-independent cytotoxic T cell priming by upregulating CD40L on dendritic cells. Immunity 30, 218–227.
Kaminski, D.A., Wei, C., Qian, Y., Rosenberg, A.F., Sanz, I., 2012. Advances in human B cell phenotypic profiling. Front. Immunol. 3, 302.
Kolev, M., Friec, G.L., Kemper, C., 2014. Complement—tapping into new sites and effector systems. Nat. Rev. Immunol..
Kuhrt, D., Faith, S.A., Leone, A., Rohankedkar, M., Sodora, D.L., Picker, L.J., Cole, K.S., 2010. Evidence of early B-cell dysregulation in simian immunodeficiency virus infection: rapid depletion of naive and memory B-cell subsets with delayed reconstitution of the naive B-cell population. J. Virol. 84, 2466–2476.
Lischke, T., Heesch, K., Schumacher, V., Schneider, M., Haag, F., Koch-Nolte, F., Mittrucker, H.W., 2013. CD38 controls the innate immune response against Listeria monocytogenes. Infect. Immun. 81, 4091–4099.
Lopes-Carvalho, T., Foote, J., Kearney, J.F., 2005. Marginal zone B cells in lymphocyte activation and regulation. Curr. Opin. Immunol. 17, 244–250.
MacKenzie, S.H., Clark, A.C., 2012. Death by caspase dimerization. Adv. Exp. Med. Biol. 747, 55–73.
Malkiel, S., Kuhlow, C.J., Mena, P., Benach, J.L., 2009. The loss and gain of marginal zone and peritoneal B cells is different in response to relapsing fever and Lyme disease Borrelia. J. Immunol. 182, 498–506.
Martin, F., Kearney, J.F., 2002. Marginal-zone B cells. Nat. Rev. Immunol. 2, 323–335.
McComb, S., Mulligan, R., Sad, S., 2010. Caspase-3 is transiently activated without cell death during early antigen driven expansion of CD8(+) T cells in vivo. PLoS One 5, e15328.
Messaoudi, I., Estep, R., Robinson, B., Wong, S.W., 2011. Nonhuman primate models of human immunology. Antioxid. Redox Signal. 14, 261–273.
Minguet, S., Dopfer, E.P., Pollmer, C., Freudenberg, M.A., Galanos, C., Reth, M., Huber, M., Schamel, W.W., 2008. Enhanced B-cell activation mediated by TLR4 and BCR crosstalk. Eur. J. Immunol. 38, 2475–2487.
Moir, S., Buckner, C.M., Ho, J., Wang, W., Chen, J., Waldner, A.J., Posada, J.G., Kardava, L., O'Shea, M.A., Kottilil, S., Chun, T.W., Proschan, M.A., Fauci, A.S., 2010. B cells in early and chronic HIV infection: evidence for preservation of immune function associated with early initiation of antiretroviral therapy. Blood 116, 5571–5579.
Moir, S., Fauci, A.S., 2009. B cells in HIV infection and disease. Nat. Rev. Immunol. 9, 235–245.
Moir, S., Ho, J., Malaspina, A., Wang, W., DiPoto, A.C., O'Shea, M.A., Roby, G., Kottilil, S., Arthos, J., Proschan, M.A., Chun, T.W., Fauci, A.S., 2008. Evidence for HIV-associated B cell exhaustion in a dysfunctional memory B cell compartment in HIV-infected viremic individuals. J. Exp. Med. 205, 1797–1805.
Moir, S., Malaspina, A., Li, Y., Chun, T.W., Lowe, T., Adelsberger, J., Baseler, M., Ehler, L.A., Liu, S., Davey Jr., R.T., Mican, J.A., Fauci, A.S., 2000. B cells of HIV-1-infected patients bind virions through CD21-complement interactions and transmit infectious virus to activated T cells. J. Exp. Med. 192, 637–646.
Muller, J., Nitschke, L., 2014. The role of CD22 and Siglec-G in B-cell tolerance and autoimmune disease. Nat. Rev. Immunol. 10, 422–428.
Oliver, A.M., Martin, F., Gartland, G.L., Carter, R.H., Kearney, J.F., 1997. Marginal zone B cells exhibit unique activation, proliferative and immunoglobulin secretory responses. Eur. J. Immunol. 27, 2366–2374.
Onu, A., Pohl, T., Krause, H., Bulfone-Paus, S., 1997. Regulation of IL-15 secretion via the leader peptide of two IL-15 isoforms. J. Immunol. 158, 255–262.
Peruchon, S., Chaoul, N., Burelout, C., Delache, B., Brochard, P., Laurent, P., Cognasse, F., Prevot, S., Garraud, O., Le Grand, R., Richard, Y., 2009. Tissue-specific B-cell dysfunction and generalized memory B-cell loss during acute SIV infection. PLoS One 4, e5966.
Peter, M.E., Budd, R.C., Desbarats, J., Hedrick, S.M., Hueber, A.O., Newell, M.K., Owen, L.B., Pope, R.M., Tschopp, J., Wajant, H., Wallach, D., Wiltrout, R.H., Zörnig, M., Lynch, D.H., 2007. The CD95 receptor: apoptosis revisited. Cell 129, 447–450.
Pillai, S., Cariappa, A., Moran, S.T., 2005. Marginal zone B cells. Annu. Rev. Immunol. 23, 161–196.
Pistoia, V., 1997. Production of cytokines by human B cells in health and disease. Immunol. Today18, 343–350.
Regidor, D.L., Detels, R., Breen, E.C., Widney, D.P., Jacobson, L.P., Palella, F., Rinaldo, C. R., Bream, J.H., Martinez-Maza, O., 2011. Effect of highly active antiretroviral therapy on biomarkers of B-lymphocyte activation and inflammation. Aids 25, 303–314.
Rodig, S.J., Jones, D., Shahsafaei, A., Dorfman, D.M., 2002. CCR6 is a functional chemokine receptor that serves to identify select B-cell non-Hodgkin's lymphomas. Hum. Pathol.33, 1227–1233.
Shen, P., Lampropoulou, V., Stervbo, U., Hilgenberg, E., Ries, S., Mecqinion, A., Fillatreau, S., 2013. Intrinsic Toll-like receptor signalling drives regulatory function in B cells. Front. Biosci. 5, 78–86.
Smith, S.H., Haas, K.M., Poe, J.C., Yanaba, K., Ward, C.D., Migone, T.S., Tedder, T.F., 2010. B-cell homeostasis requires complementary CD22 and BLyS/BR3 survival signals. Int. Immunol. 22, 681–691.
Strasser, A., Jost, P.J., Nagata, S., 2009. The many roles of FAS receptor signaling in the immune system. Immunity 30, 180–192.
Thibult, M.L., Rivals, J.P., Mamessier, E., Gertner-Dardenne, J., Pastor, S., Speiser, D.E., Derre, L., Olive, D., 2013. CpG-ODN-induced sustained expression of BTLA mediating selective inhibition of human B cells. J. Mol. Med. 91, 195–205.
Thomas, M.A., Tuero, I., Demberg, T., Vargas-Inchaustegui, D.A., Musich, T., Xiao, P., Venzon, D., LaBranche, C., Montefiori, D.C., DiPasquale, J., Reed, S.G., DeVico, A., Fouts, T., Lewis, G.K., Gallo, R.C., Robert-Guroff, M., 2014. HIV-1 CD4-induced (CD4i) gp120 epitope vaccines promote B and T-cell responses that contribute to reduced viral loads in rhesus macaques. Virology 471–473, 81–92.
Titanji, K., Velu, V., Chennareddi, L., Vijay-Kumar, M., Gewirtz, A.T., Freeman, G.J., Amara, R.R., 2010. Acute depletion of activated memory B cells involves the PD-1 pathway in rapidly progressing SIV-infected macaques. J. Clin. Invest. 120, 3878–3890.
Titanji, K., Vunnava, A., Sheth, A.N., Delille, C., Lennox, J.L., Sanford, S.E., Foster, A., Knezevic, A., Easley, K.A., Weitzmann, M.N., Ofotokun, I., 2014. Dysregulated B cell expression of RANKL and OPG correlates with loss of bone mineral density in HIV infection. PLoS Pathog. 10, e1004497.
Tsukamoto, Y., Nagai, Y., Kariyone, A., Shibata, T., Kaisho, T., Akira, S., Miyake, K., Takatsu, K., 2009. Toll-like receptor 7 cooperates with IL-4 in activated B cells through antigen receptor or CD38 and induces class switch recombination and IgG1 production. Mol. Immunol. 46, 1278–1288.
Vazquez, B.N., Laguna, T., Carabana, J., Krangel, M.S., Lauzurica, P., 2009. CD69 gene is differentially regulated in T and B cells by evolutionarily conserved promoter-distal elements. J. Immunol. 183, 6513–6521.
Victora, G.D., Mesin, L., 2014. Clonal and cellular dynamics in germinal centers. Curr. Opin. Immunol. 28, 90–96.
Vugmeyster, Y., Howell, K., Bakshi, A., Flores, C., Hwang, O., McKeever, K., 2004. B-cell subsets in blood and lymphoid organs in Macaca fascicularis. The Journal of the International Society for Analytical Cytology. Cytometry Part A 61, 69–75.
Vugmeyster, Y., Seshasayee, D., Chang, W., Storn, A., Howell, K., Sa, S., Nelson, T., Martin, F., Grewal, I., Gilkerson, E., Wu, B., Thompson, J., Ehrenfels, B.N., Ren, S., Song, A., Gelzleichter, T.R., Danilenko, D.M., 2006. A soluble BAFF antagonist, BR3-Fc, decreases peripheral blood B cells and lymphoid tissue marginal zone and follicular B cells in cynomolgus monkeys. Am. J. Pathol. 168, 476–489.
Watanabe, N., Gavrieli, M., Sedy, J.R., Yang, J., Fallarino, F., Loftin, S.K., Hurchla, M.A., Zimmerman, N., Sim, J., Zang, X., Murphy, T.L., Russell, J.H., Allison, J.P., Murphy, K.M., 2003. BTLA is a lymphocyte inhibitory receptor with similarities to CTLA-4 and PD-1. Nat. Immunol. 4, 670–679.
Weill, J.C., Weller, S., Reynaud, C.A., 2009. Human marginal zone B cells. Annu. Rev. Immunol. 27, 267–285.
Zouali, M., Richard, Y., 2011. Marginal zone B-cells, a gatekeeper of innate immunity. Front. Immunol. 2, 63.